

Original Research

View Article online



Received 27 September 2025

Revised 18 November 2025

Accepted 28 January 2026

Available Online 30 June 2026

Edited by Si Mi

## KEYWORDS:

Gelatin  
Wound healing  
Cytotoxicity  
*Cynoglossus arel*  
Chondroitin sulfate  
NHDF cells

<https://doi.org/10.53365/nrfhh/217473>

eISSN: 2583-1194

Copyright © 2026 Visagaa Publishing House

## Sustainable valorization of *Cynoglossus arel* skin waste into functional biopolymers: extraction, characterization, and biomedical applications in dermal cell regeneration

Asmita Parida<sup>1</sup>, Majesh Tomson<sup>1</sup>, K. B. Arun<sup>1,\*</sup>

<sup>1</sup>Department of Life Sciences, CHRIST (Deemed to be University), India

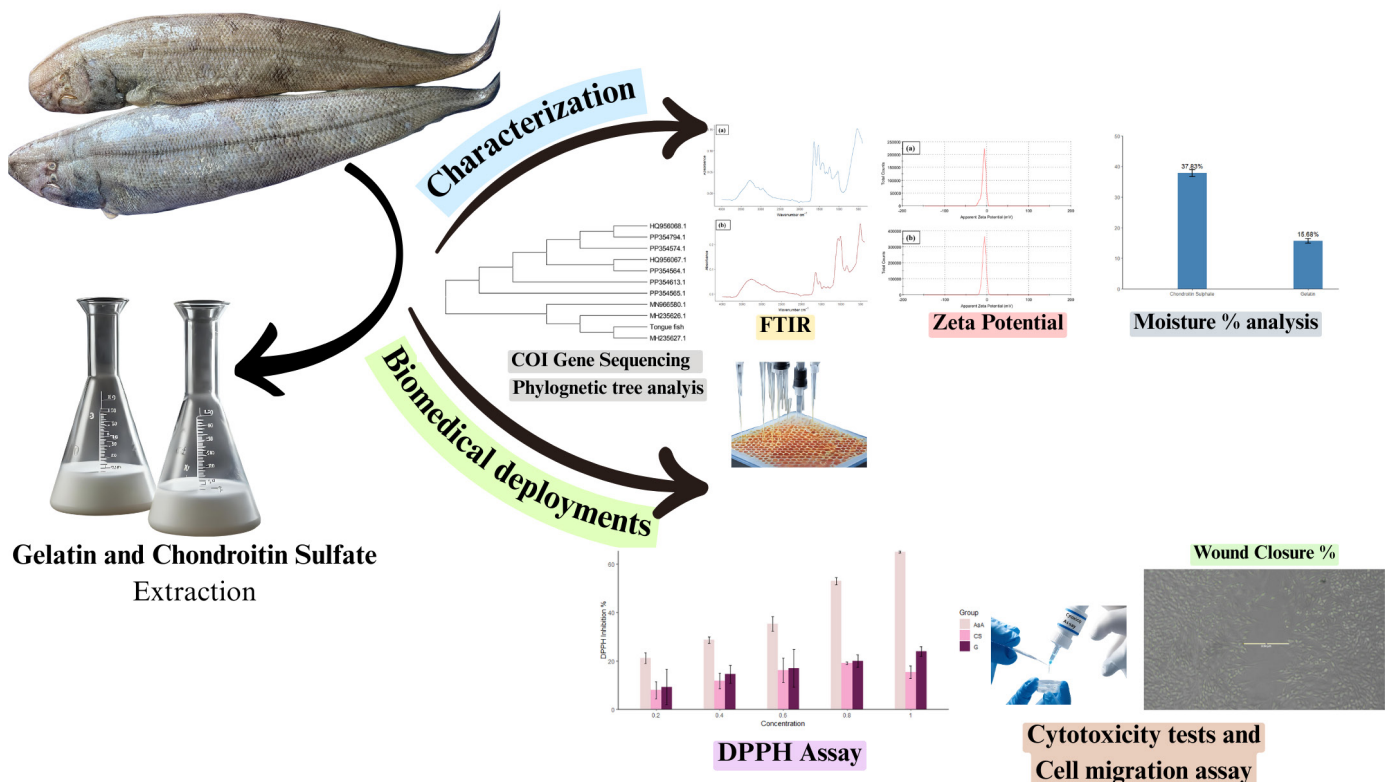
**ABSTRACT:** The growing problem of fishery waste poses a significant environmental concern and represents a valuable untapped source of biomaterials that can be converted into useful resources. This research aims to achieve the sustainable valorization of *Cynoglossus arel* waste. We extracted and characterized gelatin and chondroitin sulfate from fish skin and rigorously analyzed them to assess the integrity of their functional groups and their colloidal stability. The findings further verify that the gelatin has appropriate structure characteristics, as supported by tests for moisture content and gelation. Meanwhile, chondroitin sulfate was shown to be sulfated using Toluidine Blue, Safranin O, and Methylene Blue precipitation tests. Following their confirmatory tests, the antioxidant activities of the biopolymers were examined by the DPPH radical scavenging assay. The gelatin and chondroitin sulfate exhibited moderate antioxidant activity, suggesting their potential to combat oxidative stress. Their potential for biomedical applications, especially in wound healing, was evaluated using cell migration assays with normal human dermal fibroblast cells. When applied at specific concentrations, the biopolymer extracts significantly improved cell migration and accelerated wound healing compared with the control group. These results illuminate the high potential for utilizing *Cynoglossus arel* fish waste to produce bioactive compounds with significant therapeutic uses. The research establishes the dual advantage of valorizing marine waste and producing low-cost, natural biomaterials for regenerative medicine, especially for dermal repair.

\* Corresponding author.

E-mail address: [arun.kb@christuniversity.in](mailto:arun.kb@christuniversity.in) (K. B. Arun)

This is an open access article under the CC BY-NC-ND license (<http://creativecommons.org/licenses/by-nc-nd/4.0/>).

## GRAPHICAL ABSTRACT

Sustainable valorization of *Cynoglossus arel* skin waste

## 1. INTRODUCTION

The fish processing industry can generate significant byproducts, which include skin, scales, bones, and viscera, which are prone to underutilization despite their potential as sources of functional biopolymers (Abelti et al., 2022). *Cynoglossus arel*, the largescale tongue-sole, is a benthic flatfish of the family Cynoglossidae. The mucus-covered integument supports large, coarse ctenoid scales present on the ocular side, whereas smooth cycloid scales are present on the blind side, facilitating sediment attachment and burrowing capacity (Kishipour et al., 2023; Minicozzi et al., 2019). This species lacks pectoral and pelvic fins, which is a distinctive characteristic of *Cynoglossus*, and has continuous dorsal and anal fins, respectively (Oujifard et al., 2017; Black and Berendzen, 2020). The skin of *Cynoglossus arel* contains a large quantity of collagen and glycosaminoglycans and hence serves as a valuable raw material for the recovery of gelatin and chondroitin sulfate production (Rajabimashhadi et al., 2023).

Gelatin is a partially hydrolyzed collagen derived from acid or enzymatic hydrolysis of collagen material, like fish skin. It is a proteinaceous polymer that can form a gel, is biocompatible, and is film-forming (Das et al., 2017). Chondroitin sulfate is a sulfated glycosaminoglycan and is a basic structure of cartilage and connective tissue, which is typically derived by extracting from fish skin via alkaline or enzymatic digestion processes with further precipitation and purification treatments. Chondroitin Sulfate exhibits excellent anti-inflammatory, chondroprotective, and antioxidant activities (Medeiros et al., 2021). The simultaneous extraction of chondroitin sulfate and gelatin from the skin of *C. arel* not only imparts economic value to fish waste material but also promotes sustainable bioprocessing.

Despite published work on the extraction of gelatin from other fish sources, information on the simultaneous or sequential extraction of the two compounds from the same biomass, especially from *C. arel*, is lacking. Moreover, there is a lack of knowledge regarding comparative studies of different

extraction methods, the optimization of multiple conditions, and product quality for pharmaceutical or biomedical applications. Such a situation presents a significant opportunity for improving bioprocess development, waste valorization, and the generation of sustainable products (Bellon-Maurel et al., 2013). The primary objective of this research is to develop a productive and sustainable sequential extraction protocol for gelatin and chondroitin sulfate from *C. arel* skin, a widely underexploited flatfish species.

Following the extraction, the research anticipates determining the physicochemical properties of gelatin and chondroitin sulfate through analytical techniques such as Fourier-transform infrared spectroscopy (FTIR) (Tkachenko and Niedzielski, 2022) and zeta potential (Serrano-Lotina et al., 2023) to analyze their structural and functional properties. Finally, the research anticipates demonstrating the feasibility of using *C. arel* skin as a dual-resource material, advancing waste valorization, sustainable biomaterial production, and circular bioeconomy practice in fisheries (Nzihou, 2010). In addition to their industrial applications, gelatin and chondroitin sulfate have shown strong potential for wound healing. Gelatin supports cell adhesion and proliferation, whereas chondroitin sulfate promotes fibroblast migration, ECM remodeling, and anti-inflammatory activity (Huang et al., 2018). Together, they created a bioactive environment that can accelerate tissue repair, making them ideal candidates for developing natural wound-healing biomaterials from marine waste (Karydis-Messinis et al., 2023).

## 2. MATERIALS AND METHODS

### 2.1. Extraction of skin from *Cynoglossus arel*

The fresh specimens of *Cynoglossus arel* (approximately 1 kg) were collected from a local fishmonger in SG Palya, 12°55'34.3 "N 77°36'22.2 "E, WJG4+FFF Bengaluru, Karnataka. They were appropriately washed with distilled water to remove any debris and contaminants. The scales were carefully removed from both dorsal and ventral surfaces. The outer skin from both surfaces was peeled off carefully from the flesh using a knife and forceps. The peeled skin was again washed using distilled water to avoid contamination during further extraction. The skin was carefully removed from the fish and exposed to chemical and enzymatic treatments and tests to extract gelatin and chondroitin sulfate efficiently. These treatments were optimized to ensure maximum yield and purity. For further characterization and analysis, the skin was stored in an air-tight container at -20 °C to prevent decomposition or degradation (Wang and Regenstein, 2009).

### 2.2. Identification of species

Accurate species identification is crucial in this research as it ensures that the extracted materials are indeed from *Cynoglossus arel*. This was achieved through DNA barcoding using molecular techniques targeting the barcode gene (Knebelberger and Stöger, 2012). DNA was isolated from the fish sample. Its purity was checked using agarose gel electrophoresis. There is a distinct band for high-molecular-weight DNA in agarose gel electrophoresis. The cytochrome c oxidase subunit I (COI) gene fragment was amplified with LCO and R2 primers with a single discrete PCR amplicon. A 700 bp band was observed upon agarose gel resolution. PCR amplicon's forward and reverse DNA sequencing reaction was conducted using LCO and R2 primers with BDT v3.1 cycle sequencing kit on an ABI 3730xl Genetic analyzer. COI gene consensus sequence derived from forward and reverse sequence data with the aligner software. The COI gene sequence was used to conduct a BLAST search against the NCBI GenBank database's 'nr' database. The first 10 sequences were chosen based on the highest identity score, followed by alignment with the multiple alignment program Clustal W. The RDP program was used to compute the distance matrix database. The phylogenetic tree was specifically constructed using MEGA 11 (Soman et al., 2020). The evolutionary history was inferred by using the Maximum Likelihood method and the Tamura-Nei model. Initial tree(s) for the heuristic search were obtained automatically by applying Neighbor-Join and BioNJ algorithms to a matrix of pairwise distances estimated using the Tamura-Nei model and then selecting the topology with the superior log likelihood value (Hall, 2013; Tamura et al., 2011).

### 2.3. Extraction of gelatin

20 g of the stored fish skin sample was weighed and thoroughly rinsed with distilled water. The skin was immersed in 100 mL of 95% ethanol for 1 hour at room temperature. The sample was transferred to a fresh ethanol solution and incubated for another 1 hour. Further, the sample was washed with distilled water and blotted dry (Sen et al., 1966). Alkaline pretreatment was done to remove the non-collagenous proteins. The defatted skin was immersed in 100 mL of 0.1 N NaOH. It was incubated at room temperature for 30 minutes with constant stirring. The process was repeated and further rinsed with distilled water (Arpi et al., 2018). For collagen swelling, the alkaline-treated sample was immersed in 0.1 M acetic acid and incubated at 4 °C for 4 hours with occasional stirring, followed by washing with distilled water (See et al., 2015). The pretreated sample was immersed in 100 mL of distilled water (1:5 w/v) and incubated in a water bath maintained at

60 °C for 5 hour with occasional stirring. The gelatin filtrate was filtered through Whatman's filter paper to remove debris or contaminants (Huang et al., 2017). 20 mL of gelatin extract was evenly poured onto sterile steel plates and dried in a hot-air oven for 48 hours to obtain dried gelatin films. The remaining liquid gelatin extract was stored for further analysis and characterization (Giménez et al., 2005).

#### 2.4. Extraction of chondroitin sulfate

20 g of the stored fish skin sample was weighed and thoroughly rinsed with distilled water. The skin was defatted by immersing it in 100 mL of 95% ethanol for 1 hour at room temperature. The sample was transferred to a fresh ethanol solution and incubated for another 1 hour. Further, the sample was washed with distilled water and blotted dry (Sen et al., 1966). The defatted skin sample was enzymatically digested by incubating in phosphate buffer (100 mL) containing trypsin (200 mg) for 48 hour (Katakami et al., 1985). The digested sample was treated with 5% trichloroacetic acid and incubated for 1 hour. The incubated mixture was further centrifuged at 8000 rpm for 20 minutes. The resulting supernatant was collected (Hemker et al., 2020). The accurate volume of supernatant was measured. To this supernatant, three times the volume of ice-cold absolute ethanol was added and incubated for 24 hours at 4 °C (Nogueira et al., 2019). The incubated solution was taken and centrifuged at 8000 rpm for 20 minutes. The supernatant was discarded, and the pellet was resuspended in 10 mL of distilled water. The solution was then precipitated using double the volume of ice-cold isopropanol. This solution was incubated for 24 hour at 4 °C (Vázquez et al., 2019). The incubated sample was centrifuged at 8000 rpm for 20 minutes. The supernatant was discarded, and the pellet was collected. The pellet was resuspended in distilled water (depending on the quantity and density of the pellet obtained) (Sikder and Das, 1979). The extraction was repeated twice to obtain a higher yield of chondroitin sulfate. 10 mL of the extract was poured onto sterile steel plates and heated in a hot-air oven at 60°C for 48 hours to obtain dried chondroitin sulfate powder. The extract solution was stored for analysis and characterization tests (Hagiwara et al., 2013).

#### 2.5. Qualitative analysis of gelatin

- (i) *Gelation test* was performed by dissolving 0.2 g of dried gelatin in 10 mL of hot distilled water. It was allowed to refrigerate for 3 hour and was checked for the formation of a gel.
- (ii) *The moisture content of the gelatin* was analyzed using a moisture analyzer (SHIMADZU). Approximately 0.05 g

of gelatin was taken and evenly spread on the pan to allow even heating. The heating temperature and the moisture percentage were analyzed (Avena-Bustillos et al., 2011).

- (iii) The *protein content* in gelatin was analyzed by Lowry's method. Different volumes of a standard solution of bovine serum albumin (1 mg/mL) were pipetted, ranging from 0.04 to 0.2 mL, and diluted to 1 mL with distilled water (Redmile-Gordon et al., 2013). Similarly, 0.2 and 0.4 mL of gelatin extract were combined and diluted to 1 mL with distilled water. Freshly prepared alkaline copper reagent (5 mL) was added to all test tubes. The tubes were incubated at room temperature for 10 minutes. Soon after incubation, Folin-Ciocalteu reagent was added (0.5 mL), mixed uniformly, and incubated for 30 minutes at room temperature under dark conditions. The absorbance of all the test tubes was recorded at 660 nm (Zhou and Regenstein, 2006). The protein concentration of the test samples was analyzed by comparing their values with the standard curve (Campbell, 1983).

#### 2.6. Qualitative analysis for chondroitin sulfate

- (i) The *Toluidine test* was done by adding 1 mL of 0.05% toluidine blue solution to 1 mL of chondroitin sulfate solution (1 mg/mL) in a test tube. The tube was allowed to stand for 10 minutes at room temperature (Volpi et al., 2005; Ye et al., 2021).
- (ii) *Safranin O test*: 1 mL of chondroitin sulfate (1 mg/mL) was taken in a test tube and mixed with 1 mL of 0.1% safranin O reagent. It was appropriately mixed and allowed to stand for 10 minutes at room temperature (Mao et al., 1998).
- (iii) For the *Methylene blue precipitation test*, 1 mL of chondroitin sulfate (1mg/mL) was taken in a test tube and mixed with 1 mL of 0.1% methylene blue dye. Followed by the addition of 1 mL of 5% trichloroacetic acid (Abdelrahman et al., 2022).
- (iv) *Moisture content* was performed as described earlier for gelatin moisture content analysis. 50 mg of chondroitin sulfate was taken and evenly spread on the pan to allow even heating. The heating temperature and the moisture percentage were analyzed (Nithinkumar et al., 2022).

#### 2.7. Determination of antioxidant activity using 2,2-diphenyl-1-picrylhydrazyl (DPPH) assay

From the 1 mg/mL stock solutions of gelatin, chondroitin sulfate, and ascorbic acid, different volumes (0.2 – 1 mL) were taken, and each was made up to 1 mL with distilled

water. Then, 100  $\mu\text{L}$  of each test was transferred to a 96-well microplate, followed by 100  $\mu\text{L}$  of freshly prepared DPPH solution. A control (100  $\mu\text{L}$  methanol and 100  $\mu\text{L}$  DPPH) and a blank (100  $\mu\text{L}$  ascorbic acid and 100  $\mu\text{L}$  methanol) were used for the assay. The plate is incubated in the dark for 30 minutes with gentle shaking. The absorbance was recorded at 517 nm using a microplate reader (Krüzelyi et al., 2023). The percentage of DPPH Scavenging activity was calculated using the formula described by Flieger and Flieger (2020).

$$\% \text{ Inhibition} = \frac{A_{(\text{control})} - A_{(\text{sample})}}{A_{(\text{control})}} \times 100$$

where  $A_{(\text{control})}$  is the absorbance of DPPH + methanol,  $A_{(\text{sample})}$  is the absorbance of DPPH + sample (gelatin or chondroitin sulfate).

## 2.8. Characterization of functional groups using FTIR

Approximately 1–2 mg of the dried sample (gelatin and chondroitin sulfate) was kept directly on the ATR crystal (Attenuated Total Reflectance). The sample was pressed very gently against the crystal using the pressure arm. The background spectrum was recorded using an empty, clean crystal. The sample spectrum was then recorded with a range of 4000–400  $\text{cm}^{-1}$ , with a resolution of 4  $\text{cm}^{-1}$  and 32 scans. The spectrum was saved, and the baseline was normalized and corrected. The resulting spectrum was further analyzed for the sample's characteristic peaks (Tkachenko and Niedzielski, 2022).

## 2.9. Zeta potential analysis

Sample solutions (approximately 6 mL) of gelatin and chondroitin sulfate were formulated in deionized water at a concentration of 0.5 mg/mL. Approximately 700–1000  $\mu\text{L}$  of the sample was transferred into a clean zeta potential cell without introducing air bubbles. The zeta potential instrument (Malvern) was turned on and allowed to stabilize. The sample cell was inserted into the measurement chamber. Parameters such as temperature (approximately 25  $^{\circ}\text{C}$ ), dielectric constant, viscosity, zeta potential runs, and the dispersant measurement position were input. The instrument automatically measured electrophoretic mobility. Measurements were conducted in triplicate, and the average  $\pm$  standard deviation was reported. The measured zeta potential (mV) values were analyzed for colloidal stability behavior (Serrano-Lotina et al., 2023).

## 2.10. Cell migration studies on the normal human dermal fibroblast (NHDF) cell line

### 2.10.1. Cytotoxicity screening using NHDF cells

The cell count was standardized to  $1.0 \times 10^4$  cells/mL using the required complete culture media. To each well of the prelabelled 96-well microtiter plate, 100  $\mu\text{L}$  of the prepared cell suspension (10,000 cells/well) was added and incubated at 37  $^{\circ}\text{C}$  with 5%  $\text{CO}_2$ . After 24 hour of incubation, the supernatant was removed, and the monolayer was rinsed with plain media. To each pre-designated well, 100  $\mu\text{L}$  of test samples at various concentrations were added, and the samples were incubated for 24 hours. After incubation, the test solutions in the wells were discarded, and 100  $\mu\text{L}$  of MTT reagent (0.5 mg/mL of MTT in PBS) was added to each well. The plates were incubated for 4 hour at 37  $^{\circ}\text{C}$  in 5%  $\text{CO}_2$ . The supernatant was removed, 100  $\mu\text{L}$  of DMSO was added, and the plate was gently shaken to solubilize the formazan crystals. The absorbance readings were recorded at 590 nm using a multimode plate reader, SpectraMax i3X (Molecular Devices), according to the manufacturer's instructions (Muchová et al., 2021). The percentage growth inhibition was calculated using the given formula, with the test drug concentration required to inhibit cell growth by 50%. Values are generated from the dose-response curves of cells using GraphPad Prism 5.0 software (Malik et al., 2022).

$$\% \text{ Inhibition} = \frac{\text{OD of Control} - \text{OD of Sample}}{\text{OD of Control}} \times 100$$

### 2.10.2. Wound healing assay

With the cytotoxicity screening results, 1000 ( $\mu\text{g}/\text{mL}$ ) of gelatin solution prepared in plain media and 100 ( $\mu\text{g}/\text{mL}$ ) of chondroitin sulfate were mixed. The resulting (10:1) mixture was combined with an equal volume of medium, yielding a final test concentration containing 500 ( $\mu\text{g}/\text{mL}$ ) gelatin and 50 ( $\mu\text{g}/\text{mL}$ ) chondroitin sulfate, which was used for the migration assay (Karydis-Messinis et al., 2023). Cells were carefully detached from the tissue culture plate by 0.25% Trypsin-EDTA solution. The cells were pelleted in a 15 mL conical tube by centrifugation. The resulting supernatant was aspirated, and the cells were resuspended in culture media. A required number of cells were plated in a six-well plate to achieve 100% confluence within 24 hours. In a sterile environment, a 200  $\mu\text{L}$  pipette tip was firmly pressed against the top of the tissue culture plate, and a vertical wound was swiftly created through the cell monolayer (the scratch created was approximately 2  $\mu\text{m}$  wide). Excessive force was avoided to prevent damage to the tissue culture surface. The media and cell debris were carefully aspirated. Fresh culture

media containing the desired concentrations of test samples was slowly added along the side wall of the well to ensure complete coverage of the well bottom and to prevent further cell detachment. Following wound creation and inspection, an initial image was captured. The plate was then incubated at 37 °C with 5% CO<sub>2</sub>. At several time points (e.g., every 24 hours), the plate was removed from the incubator and placed under an inverted microscope. Images were taken to monitor wound closure. The time required for wound closure varied depending on the cell type (Pijuan et al., 2019).

The distance between the wound's edges was measured using a scale bar in ImageJ software for analysis. The progression of wound closure over time was analyzed and presented graphically using bar plots. The wound healing/closure was calculated using the given formula (Gould et al., 2022):

Wound closure % =

$$\frac{\text{Migration Dist. at 0 hours} - \text{Migration Dist. at Time } t}{\text{Migration Dist. at 0 hours}} \times 100$$

### 3. RESULTS

#### 3.1. Confirmation of *Cynoglossus* species

A sample, which was labeled as Tongue fish (Figure 1), might be *Cynoglossus arel*, and showed high similarity based on nucleotide homology and phylogenetic analysis (Hall, 2013; Tamura et al., 2011).

**Extraction of skin:** The skin yield obtained from 1 kg of the fish sample was 80.925 g.

**Gelatin extraction:** From 20 g of fish skin sample, approximately 100 mL of gelatin filtrate was obtained. From this 100 mL, 20 mL of gelatin filtrate was dried, and the dry weight of the gelatin films was obtained as approximately 0.320 g.

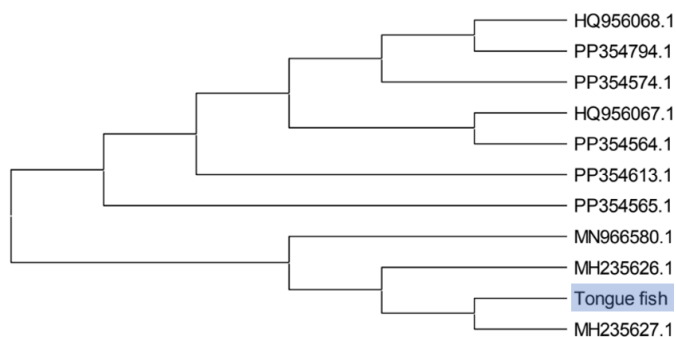


**Figure 1.** The phylogenetic tree with the highest log likelihood (-1037.88) is shown for Tongue Fish.

The remaining filtrate is stored at 4 °C for further analysis and tests. Gelatin yield was calculated for a 20 g skin sample at 8%.

**Chondroitin sulfate extraction:** From 20 g of fish skin sample, approximately 29 mL of chondroitin sulfate was obtained. From this 29 mL, 20 mL of chondroitin sulfate solution was dried, and the resulting powder weighed approximately 0.650 g. Another 25 mL of extract solution was obtained, as the extraction was repeated twice. The remaining extract was stored at 4 °C for further analysis and tests.

#### 3.2. Qualitative analysis for gelatin

Upon refrigeration at 4 °C for 4 hour, the solution formed a firm, transparent gel, indicating intact gel-forming proteins and triple-helix reformation. The gel exhibited typical thermoreversible behavior, returning to a liquid state upon reheating (Avena-Bustillos et al., 2011; Wu et al., 2023). The moisture % for 0.05 g of gelatin was recorded as 15.68 ± 0.784% as the temperature increased from room temperature (25 °C) to 116 °C (Nithinkumar et al., 2022), as shown in Figure 3. The protein concentration of the gelatin was determined by the Lowry method, with BSA as the standard. A standard calibration curve was plotted in the 20–200 µg/mL concentration range, exhibiting a linear correlation with an R<sup>2</sup> value of 0.9958 (Campbell, 1983). The 0.2 mg/mL gelatin solution yielded a protein concentration of 0.116 mg/mL, while the 0.4 mg/mL solution gave 0.156 mg/mL (as shown in Figure 2). These values indicate recovery efficiencies of 58% and 39%, respectively, suggesting that the extracted gelatin retained a substantial amount of soluble protein, although slightly lower than expected based on the nominal concentration (Zhou and Regenstein, 2006).

0.2 mg/mL gelatin → 0.116 mg/mL measured (58% recovery)

0.4 mg/mL gelatin → 0.156 mg/mL measured (39% recovery)

The **response ratio** should be:

- Expected: 0.156/0.116 = 1.34 (close to linear would be ~2.0)
- This **34% increase** for doubling concentration indicates significant non-linearity (Peterson, 1979).

**Response Factor Calculation:**

- At 0.2 mg/mL: Response factor = 0.116/0.2 = 0.58
- At 0.4 mg/mL: Response factor = 0.156/0.4 = 0.39

This indicates a 33% decrease in the response factor with concentration doubling.

For nominal gelatin solutions of 0.2 mg/mL and 0.4 mg/mL, the Lowry protein assay produced concentrations of 0.116 mg/mL and 0.156 mg/mL, respectively. The concentration-dependent underestimate feature of

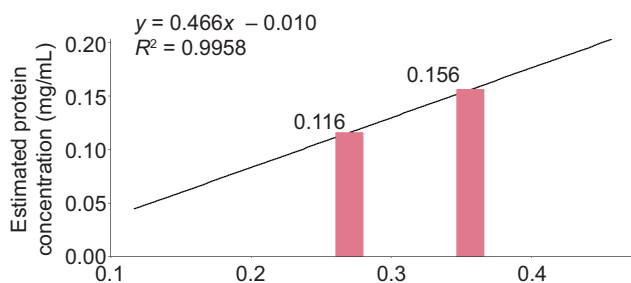


**Figure 2.** BSA standard curve with estimated protein in 0.2 and 0.4 mg/mL of gelatin as 0.116 mg/mL and 0.156 mg/mL, respectively.

gelatin quantification using BSA standards is indicated by the non-proportional rise (1.34-fold vs. predicted 2-fold) (Bera et al., 2020; Peterson, 1979). This pattern is characteristic of gelatin in the Lowry assay due to limited aromatic amino acid content (Ibrahim et al., 2011) and concentration-dependent conformational effects (Gornall and Terentjev, 2008).

### 3.3. Qualitative analysis for Chondroitin Sulfate

The detection of chondroitin sulfate in the extracted sample was confirmed using the Toluidine Blue metachromatic dye-binding assay. Upon addition of 0.05% Toluidine Blue solution to the chondroitin sulfate sample, a distinct purple-to-bluish violet coloration was observed, indicative of metachromasia (Volpi et al., 2005). Upon addition of 0.1% aqueous Safranin O solution to it, a reddish-orange coloration was observed, which revealed the association of the cationic dye with the anionic sulfate groups of chondroitin sulfate (Mao et al., 1998). The Methylene Blue precipitation test was performed to detect the prevalence of sulfated glycosaminoglycans. When chondroitin sulfate solution was mixed with 0.1% Methylene Blue solution, a distinct blue precipitate was formed within a few minutes (Abdelrahman et al., 2022). The moisture% for 0.05 g of chondroitin sulfate was recorded as  $37.83 \pm 1.1349\%$  as the temperature increased from room temperature up to  $114^\circ\text{C}$  (Nithinkumar et al., 2022, as shown in Figure 3).

### 3.4. DPPH analysis

The antioxidant potential of the extracted gelatin and chondroitin sulfate was evaluated using the DPPH radical scavenging assay (Saftić Martinović et al., 2023).

All three groups showed a general increase in DPPH inhibition percentage with increasing concentration, demonstrating dose-dependent antioxidant behavior. The average DPPH

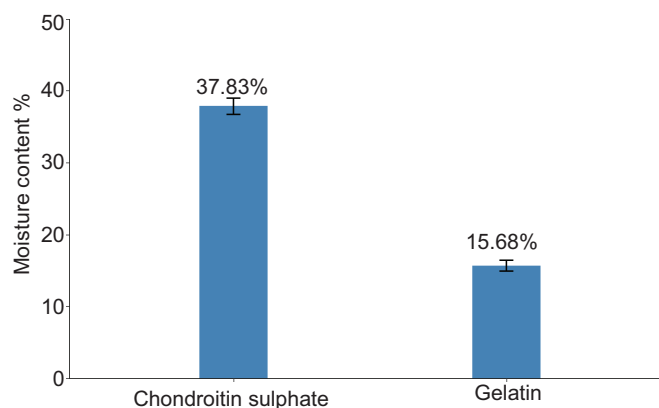


**Figure 3.** Moisture content (%) of gelatin and chondroitin sulfate.

inhibition percentage for ascorbic acid at 1 mg/mL was  $65.092 \pm 0.371\%$ . Ascorbic acid showed the highest scavenging efficacy at all concentrations. At 1.0 mg/mL, inhibition exceeds 60%, with minimal error, indicating strong and consistent antioxidant capacity. The average DPPH inhibition percentage at 1 mg/mL for chondroitin sulfate was recorded as  $15.38 \pm 2.59\%$ . Chondroitin sulfate exhibited moderate antioxidant activity, increasing gradually from ~10% at 0.2 mg/mL to ~22–24% at 1.0 mg/mL. The increase is linear and consistent, supporting its functional potential as a mild antioxidant. The average DPPH inhibition % at 1 mg/mL for gelatin was recorded as  $23.89 \pm 3.21\%$ . Gelatin showed lower inhibition values than chondroitin sulfate at all concentrations, except at 0.4 mg/mL, where both were nearly equal. The inhibition plateaus around ~20% at 1.0 mg/mL, suggesting a weaker antioxidant profile than chondroitin sulfate. Chondroitin sulfate and gelatin show larger standard deviations at intermediate concentrations (e.g., 0.6 mg/mL), which may reflect variability in solubility, reaction kinetics, or replicate measurements (Tekle et al., 2022) (as shown in Figure 4).

### 3.5. FTIR analysis

FTIR spectroscopy confirmed the detection of characteristic functional groups in the extracted gelatin and chondroitin sulfate, giving functional peaks (Nandiyanto et al., 2019; Tkachenko and Niedzielski, 2022). The FTIR spectrum of gelatin displayed distinct peaks corresponding to protein-specific vibrational modes (Al-Saidi et al., 2012; Hidayati et al., 2021). The FTIR spectrum of chondroitin sulfate showed characteristic peaks indicative of sulfated glycosaminoglycans (Thomas et al., 2021). The graphs for both groups are shown in Figure 5.

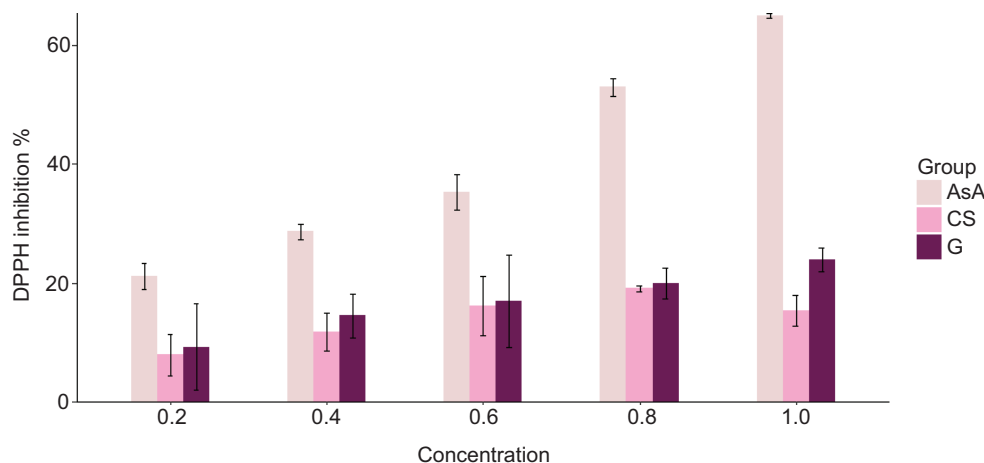


**Figure 4.** Inhibition% of ascorbic acid (AsA), chondroitin sulfate (CS), and gelatin (G).

### 3.6. Zeta potential analysis

Zeta potential was performed to assess the extracted biopolymer solutions' surface charge and colloidal stability (Serrano-Lotina et al., 2023). The Zeta potential of gelatin was obtained as  $-6.92$  mV with the zeta deviation of  $4.67$  mV and conductivity as  $0.248$  mS/cm (Cheng et al., 2023). Meanwhile, the zeta potential of chondroitin sulfate was obtained at  $-6.35$  mV, with the zeta deviation at  $4.21$  mV and the conductivity at  $0.354$  mS/cm (da Silva et al., 2012).

### 3.7. Cytotoxicity screening using NHDF cells

To determine the vitality of NHDF cells in response to test samples, cells were incubated for 24 hours with test samples at a wide range of concentrations. Cell viability was studied using the MTT assay (Muchová et al., 2021; Gonçalves et al., 2022). The control group showed 0% mean inhibition, whereas gelatin showed  $4.60 \pm 0.90\%$  at  $1$  mg/mL, and chondroitin sulfate showed  $4.82 \pm 1.09\%$  at  $0.1$  mg/mL. Cytotoxicity data on the cells are tabulated in Table 3. Samples did not show toxicity for the tested concentrations.

### 3.8. Wound healing assay

Table 4 presents data on the migration distance and wound-closure percentage for cells treated with different compounds. The control group has a migration distance of  $1.93$   $\mu$ m at 0 h, which decreases to  $0.87$   $\mu$ m at 24 hour and  $0.66$   $\mu$ m at 48 hour (as observed in Figure 7). The corresponding wound closure percentages are  $54.92\%$  at 24 hours and  $65.80\%$  at 48 hours. In contrast, the group treated

with gelatin + chondroitin sulfate ( $500$   $\mu$ g/mL +  $50$   $\mu$ g/mL) shows a migration distance of  $1.92$   $\mu$ m at 0 hours, decreasing to  $0.74$   $\mu$ m at 24 hour and  $0.54$   $\mu$ m at 48 hour (Karydis-Messinis et al., 2023) (as observed in Figure 7). The wound closure percentages for this group are  $61.46\%$  at 24 hour and  $71.88\%$  at 48 hour (Badawi et al., 2022; Gould et al., 2022).

The migration distance decreases over time for both groups. The percentage of wound closure increases over time in both groups. The group treated with gelatin + chondroitin sulfate shows a higher wound closure percentage than the control group at both 24 and 48 hour (Figure 7).

## 4. DISCUSSION

There was a recovery of  $80.93$  g of skin per 1 kg of *Cynoglossus arel*, which accounts for a skin yield of  $8.09\%$  (w/w). Remarkably, the present study demonstrates the efficient coextraction of gelatin and chondroitin sulfate from this single skin source, showcasing the high functional potential of fish skin as a versatile raw material. From  $20$  g of *Cynoglossus arel* skin, the extraction process yielded approximately  $100$  mL of gelatin filtrate, from which  $0.320$  g of dry gelatin film was recovered by drying  $20$  mL of the extract. This corresponds to an estimated gelatin content of  $1.6\%$  (w/v) in the filtrate and  $0.016$  g of gelatin per gram of raw skin, which is comparable to values reported for tropical and cold-water fish species (Gómez-Guillén et al., n.d.). The relatively modest dry weight yield is likely influenced by species-specific collagen content, extraction temperature, and time. The extraction of chondroitin sulfate (CS) from  $20$  g of *Cynoglossus arel* skin resulted in approximately  $29$  mL of CS-rich solution, from which  $0.650$  g of dry CS powder was obtained upon drying  $20$  mL of the extract. This corresponds to a  $3.25\%$  (w/v)

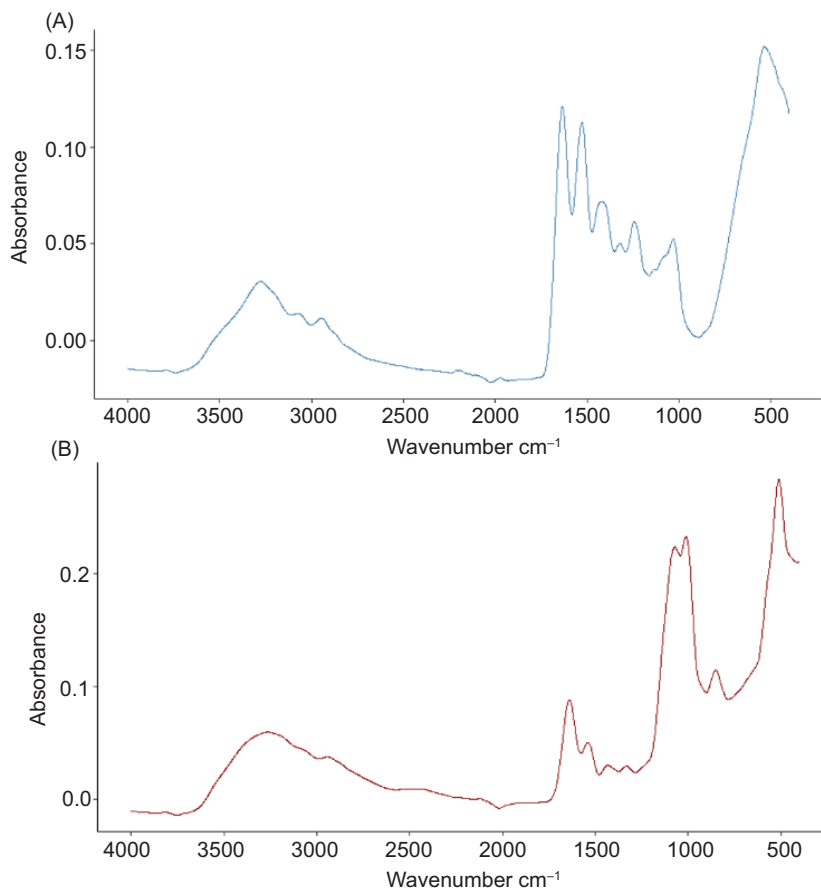


**Figure 5.** FTIR Spectrum of (A) gelatin and (B) chondroitin sulfate with functional group peaks.

**Table 1**

FTIR peaks Interpretation for gelatin and chondroitin sulfate (as shown in Figure 5).

| Wavenumber (cm <sup>-1</sup> ) | Functional group/vibration mode          | Interpretation  |
|--------------------------------|--|---|
| <b>Gelatin</b>                 |  |   |
| ~3300                          | N–H stretching (Amide A)                 | H-bonded amine groups; protein backbone                                     |
| ~3080                          | C–H asymmetric stretching (Amide B)      | CH <sub>2</sub> groups in peptide structure                                 |
| 1640–1660                      | C=O stretching (Amide I)                 | Backbone carbonyl groups are sensitive to protein conformation              |
| 1540–1555                      | N–H bending + C–N stretching (Amide II)  | Secondary amide group; protein integrity                                    |
| 1450–1400                      | CH <sub>2</sub> bending                  | Indicates the presence of methylene side chains                             |
| 1300–1230                      | N–H bending + C–N stretching (Amide III) | Complex peptide vibrations  |
| 1080–1030                      | C–O stretching                           | Possible carbohydrate residues or collagen glycosylation                    |
| <b>Chondroitin sulphate</b>    |  |   |
| ~3400                          | O–H stretching (broad)                   | Hydroxyl groups from polysaccharide chains                                  |
| ~2900                          | C–H stretching                           | Aliphatic backbone vibrations of sugar residues                             |
| 1610–1650                      | C=O stretching                           | Carboxylate groups from glucuronic acid units                               |
| 1260–1220                      | S=O asymmetric stretching                | Sulfate ester groups (–SO <sub>3</sub> <sup>-</sup> ), characteristic of CS |
| 1150–1000                      | C–O–C and C–OH stretching                | Glycosidic linkage and sugar ring vibrations                                |
| ~850–880                       | S–O symmetric stretching                 | Confirms the presence of sulfate in glycosaminoglycan chains                |

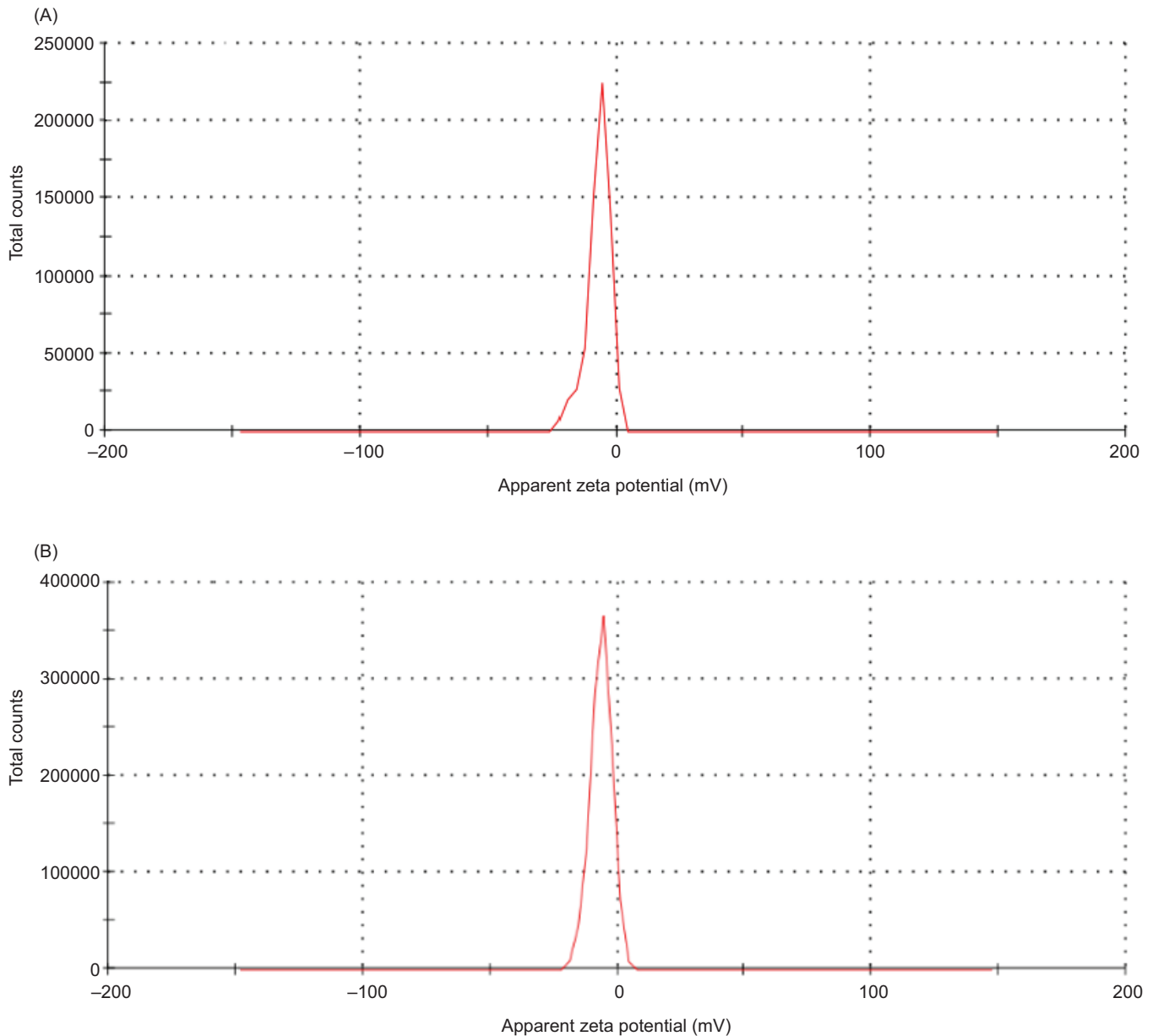


**Figure 6.** Zeta potential distribution graph for gelatin and chondroitin sulfate.

concentration of chondroitin sulfate in the solution and an approximate yield of 0.0325 g Chondroitin Sulfate per gram of raw skin. An additional 25 mL of extract was obtained through a second extraction cycle, suggesting that repetitive extraction enhances overall recovery and minimizes residual bioactive loss in discarded residues (Nogueira et al., 2019; Seixas et al., 2020).

The gelatin extracted from *Cynoglossus arel* skin exhibited characteristic gelation behavior, forming a firm and transparent gel after refrigeration at 4 °C for 4 hour. This indicates the presence of intact gel-forming proteins and partial reformation of the collagen mimetic triple-helical conformation upon cooling. The gel also exhibited thermally reversible behavior,

which liquefied upon reheating, a well-defined feature of gelatin. Such properties are crucial for biomedical and food applications where reversible sol-gel transitions are needed (Boran and Regenstein, 2010; Wu et al., 2023). The moisture content of the dried gelatin was measured at 15.68% for 0.05 g, monitored over a temperature increase from 25 °C (room temperature) to 116 °C. This value falls within the expected range (8–16%) reported for fish-derived gelatins, indicating efficient dehydration without thermal degradation. Moisture analysis is essential for understanding gelatin shelf life, stability, and film-forming ability, particularly when intended for use in pharmaceutical applications (Nithinkumar et al., 2022; Wang et al., 2023). Protein quantification, which was

**Table 3**

Cytotoxicity data for gelatin and chondroitin sulfate

| Test samples        | Conc. ( $\mu\text{g/mL}$ ) | NHDF         |              |             |              | Mean % inhibition | SD   | IC <sub>50</sub>   |
|---------------------|----------------------------|--------------|--------------|-------------|--------------|-------------------|------|--|
|                     |                            | n = 1        |              | n = 2       |              |                   |      |  |
|                     |                            | OD at 590 nm | % Inhibition | OD at 590nm | % Inhibition |                   |      |  |
| Control             | 0                          | 0.766        | 0.00         | 0.752       | 0.00         | 0.00              | 0.00 | -  |
| Gelatin             | 62.5                       | 0.756        | 1.33         | 0.746       | 0.83         | 1.08              | 0.36 | IC <sub>50</sub> not calculated due to lesser inhibition |
|                     | 125                        | 0.745        | 2.72         | 0.722       | 3.96         | 3.34              | 0.88 |  |
|                     | 250                        | 0.741        | 3.24         | 0.726       | 3.47         | 3.35              | 0.16 |  |
|                     | 500                        | 0.742        | 3.11         | 0.716       | 4.83         | 3.97              | 1.21 |  |
|                     | 1000                       | 0.726        | 5.24         | 0.722       | 3.96         | 4.60              | 0.90 |  |
| Chondroitin sulfate | 6.25                       | 0.752        | 1.88         | 0.746       | 0.86         | 1.37              | 0.72 |  |
|                     | 12.5                       | 0.749        | 2.22         | 0.735       | 2.26         | 2.24              | 0.03 |  |
|                     | 25                         | 0.742        | 3.13         | 0.728       | 3.19         | 3.16              | 0.04 |  |
|                     | 50                         | 0.739        | 3.52         | 0.722       | 3.99         | 3.76              | 0.33 |  |
|                     | 100                        | 0.735        | 4.05         | 0.710       | 5.59         | 4.82              | 1.09 |  |

**Table 4**

Wound closure % of control, gelatin, and chondroitin sulfate.

| Test compounds                | Test conc.                                    | Migration distance in $\mu\text{m}$ |      |      | % Wound Closure at |       |
|-------------------------------|---|-------------------------------------|------|------|--------------------|-------|
|                               |   | 0 h                                 | 24 h | 48 h | 24 h               | 48 h  |
| Control                       | 0   | 1.93                                | 0.87 | 0.66 | 54.92              | 65.80 |
| Gelatin + chondroitin sulfate | (500 $\mu\text{g/mL}$ + 50 $\mu\text{g/mL}$ ) | 1.92                                | 0.74 | 0.54 | 61.46              | 71.88 |

done using the Lowry's method, showed that the 0.2 mg/mL gelatin solution yielded a protein concentration of 0.116 mg/mL, while the 0.4 mg/mL solution yielded 0.156 mg/mL, which corresponded to recovery efficiencies of 58% and 39%, respectively. This suggested that a substantial portion of soluble protein remained detectable after extraction and processing. However, the lower protein concentration in the more concentrated solution may indicate protein aggregation, partial denaturation, or interference due to residual impurities or non-protein components affecting assay sensitivity (Pomory, 2008; Redmile-Gordon et al., 2013; Zhou and Regenstein, 2006). The unusual amino acid composition of gelatin, especially its low tryptophan content and low tyrosine levels compared to BSA standards (Ibrahim et al., 2011), is responsible for the non-linear relationship between actual gelatin concentration and the Lowry assay response (Legler et al., 1985). Compared with conventional proteins, the Lowry assay's reliance on aromatic amino acids for colour formation in the Folin-Ciocalteu reaction results in noticeably lower response factors for gelatin (0.39–0.58) (Bera et al., 2020). The observed nonlinearity may also be caused

by concentration-dependent conformational changes, such as partial triple-helix formation and aggregation at higher concentrations (Gornall and Terentjev, 2008), which may reduce peptide bond accessibility to copper ions in the biuret reaction. These findings underscore the need to use gelatin-specific standard curves or alternative quantitative methods, such as the hydroxyproline assay, for accurate gelatin quantification (Neuman and Logan, n.d.).

The identity of the extracted biopolymer as chondroitin sulfate (CS) was confirmed through multiple qualitative dye-based assays. The Toluidine Blue test produced a characteristic purple-to-bluish violet colour upon interaction with the sample, indicating metachromasia—a hallmark of sulfated glycosaminoglycans (GAGs). This dye adheres to polyanionic sites present on sulfated polymers, causing a spectral shift, and has long been used as a reliable colorimetric indicator for CS detection (Volpi et al., 2005). The Safranin O test resulted in a reddish-orange colour, consistent with the binding of cationic dyes to anionic sulfate and carboxyl groups, further confirming the presence of sulfated polysaccharide structures (Mao et al., 1998). Additionally, the

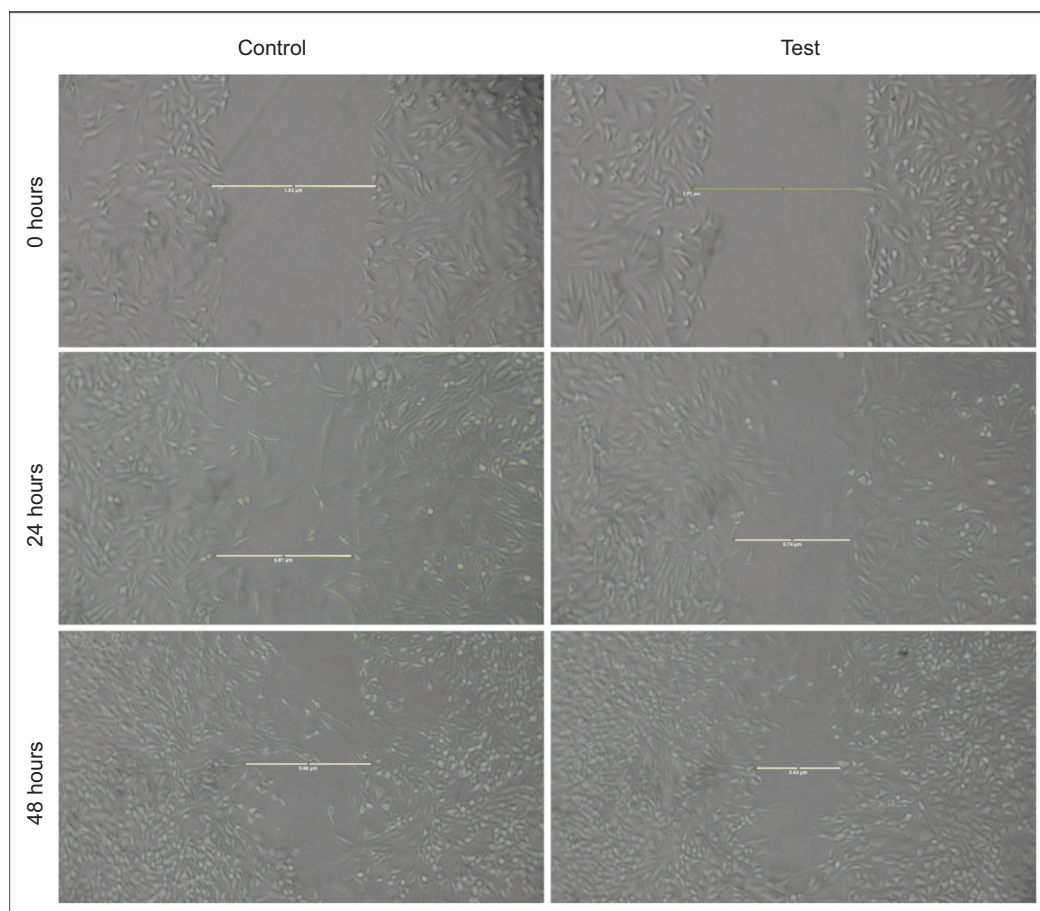


**Figure 7.** Wound closure distance at 0, 24, and 48 hour of control and test (gelatin + chondroitin sulfate).

Methylene Blue precipitation assay resulted in a distinct blue precipitate within minutes, affirming the presence of sulfated GAGs through ionic cross-linking and visible aggregation (Abdelrahman et al., 2022). The moisture content of the dry chondroitin sulfate powder was determined to be 37.83% for 0.05 g of sample, measured over a temperature ramp from 25 °C to 116 °C. The relatively high moisture value is characteristic of hygroscopic marine-derived polysaccharides, which readily retain water due to the presence of hydrophilic nature and sulfated functional groups (Nithinkumar et al., 2022).

Gelatin and chondroitin sulfate showed a dose-dependent increase in DPPH radical inhibition, confirming concentration-dependent antioxidant activity. Ascorbic acid displayed the peak scavenging performance at varying concentrations, exceeding 60% inhibition at 1.0 mg/mL, validating its strong antioxidant capacity (Saftić Martinović et al., 2023). Chondroitin sulfate exhibits moderate antioxidant activity, increasing from ~10% at 0.2 mg/mL to ~24% at 1.0 mg/mL. This consistent rise indicates its potential as a mild, functional antioxidant. In contrast, gelatin showed lower inhibition, plateauing around 20% at higher concentrations. Though gelatin

had activity comparable to CS at 0.4 mg/mL, it remained generally weaker, reflecting its limited radical-scavenging ability. These findings suggest that chondroitin sulfate has a stronger antioxidant profile than gelatin and could be helpful in mild antioxidant applications (Shiao et al., 2021).

The structural integrity and functional groups of the extracted gelatin and chondroitin sulfate (CS) were confirmed using Fourier Transform Infrared (FTIR) spectroscopy. In the gelatin spectrum, characteristic proteinaceous bands were observed: Amide A ( $\sim 3300\text{ cm}^{-1}$ ) due to N–H stretching, Amide B ( $\sim 3080\text{ cm}^{-1}$ ) from  $-\text{CH}_2$  asymmetric stretching, and a prominent Amide I band ( $1640\text{--}1660\text{ cm}^{-1}$ ) corresponding to C=O stretching of the peptide backbone, indicative of partial triple-helix retention. The Amide II ( $1540\text{--}1555\text{ cm}^{-1}$ ) and Amide III ( $1230\text{--}1300\text{ cm}^{-1}$ ) peaks further confirmed the presence of N–H bending and C–N stretching vibrations typical of collagen-derived gelatin. Additional peaks near  $1450\text{--}1400\text{ cm}^{-1}$  and  $1080\text{--}1030\text{ cm}^{-1}$  corresponded to  $\text{CH}_2$  bending and C–O stretching, respectively, supporting the presence of residual glycoproteins or glycosylation (Al-Saidi et al., 2012; Hidayati et al., 2021). For chondroitin

sulfate, broad O–H stretching around  $\sim 3400\text{ cm}^{-1}$  and C–H stretching near  $2900\text{ cm}^{-1}$  were detected, characteristic of its polysaccharide backbone. The C=O stretching band ( $1610\text{--}1650\text{ cm}^{-1}$ ) indicated carboxylate groups from glucuronic acid residues. The presence of an intense S=O asymmetric stretch ( $1220\text{--}1260\text{ cm}^{-1}$ ) confirmed the presence of sulfate groups, a key feature distinguishing Chondroitin Sulfate from other neutral GAGs. The C–O–C and C–OH vibrations ( $1000\text{--}1150\text{ cm}^{-1}$ ) represented the polysaccharide fingerprint region, and a peak around  $850\text{--}880\text{ cm}^{-1}$  that corresponded to S–O symmetric stretching, affirming the sulfation pattern (Konovalova et al., 2020). Hence, the FTIR profiles were analyzed based on previous reports, including fish-derived gelatin and marine-source chondroitin sulfate, validating the chemical identity, functional group preservation, and extraction success from *C. arel* skin. These results further support the biocompatibility and biomedical relevance of the recovered biopolymers (Nandiyanto et al., 2019; Tkachenko and Niedzielski, 2022).

The zeta potential of gelatin extracted from *C. arel* was recorded at  $-6.92\text{ mV}$ , while that of chondroitin sulfate was  $-6.35\text{ mV}$ , with corresponding zeta deviations of  $4.67\text{ mV}$  and  $4.21\text{ mV}$ , and conductivities of  $0.248\text{ mS/cm}$  and  $0.354\text{ mS/cm}$ , respectively (Oliveira et al., 2019). These negative values reflect the anionic nature of both biopolymers in aqueous solution, owing to ionizable groups such as carboxyl, amino, and sulfate groups in their molecular structures. Zeta potentials in the range of  $-6\text{ mV}$  suggest moderate colloidal stability, where the electrostatic repulsion is sufficient to maintain dispersion but may allow for some aggregation under storage or processing. The slightly higher conductivity and lower magnitude of zeta potential in chondroitin sulfate likely result from its higher sulfate group density, which increases ionic mobility and interfacial charge interactions (Ribeiro et al., 2014). These measurements confirm that both extracts retain surface-active functional groups capable of interacting with charged environments—an essential feature for their use in drug administration, tissue regeneration scaffolds, and dermal healing materials (Serrano-Lotina et al., 2023).

The selected concentrations of  $1000\text{ }\mu\text{g/mL}$  gelatin and  $100\text{ }\mu\text{g/mL}$  chondroitin sulfate for the scratch assay were based on literature-supported ranges that are nontoxic and bioactive for dermal fibroblast applications. Gelatin, as a denatured collagen derivative, is typically used in concentrations ranging from  $100$  to  $1000\text{ }\mu\text{g/mL}$  to promote cell adhesion, migration, and matrix support in vitro (Gómez-Guillén et al., n.d.). A  $500\text{ }\mu\text{g/mL}$  mid-range value ensures optimal structural and biochemical support without risking gelation or medium thickening, which can interfere with microscopy and cell mobility (Gómez-Guillén et al., n.d.). On the other hand, chondroitin sulfate exhibits anti-inflammatory activity

at relatively low concentrations ( $10\text{--}100\text{ }\mu\text{g/mL}$ ). A concentration of  $50\text{ }\mu\text{g/mL}$  of chondroitin sulfate was chosen to provide functional support in wound healing without causing osmotic imbalance or altering pH, which can affect cell health (Soltani et al., 2023). Moreover, the 10:1 gelatin-to-CS ratio also reflects the natural composition and structure of the extracellular matrix, where gelatin provides a structural framework and CS regulates signaling and hydration. This concentration pair was also validated through pre-assay cytocompatibility screening, confirming no cytotoxicity to NHDF cells (Jardim et al., 2020). The final blend thus represents a biologically relevant and safe dosage suitable for evaluating synergistic effects on fibroblast migration and wound closure (Pezeshki-Modaress et al., 2017).

The wound-healing assay demonstrated that the biopolymer blend of gelatin and chondroitin sulfate, derived from *Cynoglossus arel* skin waste, significantly enhanced fibroblast migration and wound closure compared to the untreated control (Huang et al., 2018). In the given control group, the initial wound gap of  $1.93\text{ }\mu\text{m}$  progressively decreased to  $0.87\text{ }\mu\text{m}$  at 24 h and  $0.66\text{ }\mu\text{m}$  at 48 h, reflecting wound closure percentages of 54.92% and 65.80%, respectively (Figure 7). These values represent the natural regenerative capability of NHDF cells under standard conditions without bioactive stimuli. In contrast, cells treated with the gelatin ( $500\text{ }\mu\text{g/mL}$ ) and chondroitin sulfate ( $50\text{ }\mu\text{g/mL}$ ) mixture displayed a faster healing response. The migration distance decreased from  $1.92\text{ }\mu\text{m}$  at 0 hours to  $0.74\text{ }\mu\text{m}$  at 24 hours and  $0.54\text{ }\mu\text{m}$  at 48 hours, corresponding to 61.46% and 71.88% wound closure, respectively (Figure 7). These improvements recommend studies on the fact that the biopolymer combination enhances cellular motility, likely through synergistic effects of gelatin's structural support and chondroitin sulfate's bio functional signaling. The extracted gelatin not only targets integrin-binding domains but also facilitates fibroblast adhesion and spreading (Huang et al., 2018), whereas chondroitin sulfate enhances cell proliferation, migration, and ECM remodeling, which are essential for tissue regeneration. Importantly, these results highlight the biomedical potential of underutilized marine processing waste materials. The fish skin, which is often discarded during filleting operations, was efficiently valorized into two functional biopolymers in this study. The successful extraction and application of gelatin and chondroitin sulfate from a single raw material source reduces environmental burden and exemplifies a circular bioeconomy approach, transforming waste into value-added bioactive ingredients for regenerative medicine (Rocha-Pimienta et al., 2023). The observed wound healing enhancement reinforces the viability of such biopolymer blends as cost-effective, natural alternatives to synthetic wound care agents. Future work may explore their incorporation into hydrogels, dressings,

or scaffold systems for advanced wound therapy (Pezeshki-Modaress et al., 2017).

Fish skin from *Cynoglossus arel* is traditionally underutilized and discarded during processing, yet it is rich in type I collagen and contains measurable amounts of sulfated glycosaminoglycans, such as chondroitin sulfate. The successful recovery of these two biopolymers from the same tissue demonstrates a cost-effective, resource-efficient approach for marine waste valorization (Nzihou, 2010). By converting skin waste into potential biomaterials with proven antioxidant and wound-healing properties, the study offers a crucial, sustainable approach to enhancing the economic and therapeutic value of fishery by-products, particularly from underutilized species like *C. arel* (Rocha-Pimienta et al., 2023).

## 5. CONCLUSION

The skin of *Cynoglossus arel*, an underutilised marine byproduct, was effectively used to extract and characterise gelatin and chondroitin sulphate. The integrity and functional properties of these biopolymers were validated through physicochemical analyses. The chondroitin sulphate extract contained sulfated glycosaminoglycans, according to dye-binding tests. Chondroitin sulphate was the most effective scavenger of DPPH radicals among these biopolymers, which showed mild to moderate antioxidant activity. A gelatin-chondroitin sulphate blend significantly enhanced fibroblast migration and prolonged wound healing in the NHDF cell line, indicating its biocompatibility and potential for regenerative medicine. By converting fish skin into potent wound-healing agents and encouraging sustainable resource use, this study highlights the importance of valorising marine waste. The unique characteristics and processes of these biopolymers for medicinal applications require further research.

## STATEMENTS AND DECLARATIONS

### COMPETING INTERESTS

The authors declare that there are no conflicts of interest, financial or otherwise, associated with this work.

### FUNDING

This research was conducted without external financial support from any public or private funding agency.

## AUTHOR CONTRIBUTIONS

Asmita Parida: Conceptualization, methodology, investigation, data analysis, and the original draft preparation. Majesh Tomson: Conceptual support, critical review, and manuscript validation. Arun K. B: Supervision, project administration, data interpretation, review, and editing of the manuscript.

## ACKNOWLEDGMENTS

The first author conveys her appreciation to Mr. John Merston (Ph.D. Scholar) for his extended help and guidance throughout the research. The wound healing assay was carried out with technical support and instrumentation provided by Skanda Lifesciences Laboratory, Bangalore, which the authors gratefully acknowledge. The COI gene sequencing was carried out by Barcode Biosciences, Bangalore, which the authors acknowledge.

## ETHICS APPROVAL

This study did not involve any experiments on human participants or live animals.

## DATA AVAILABILITY

All data generated or analyzed during this study are available from the corresponding author upon reasonable request.

## ORCID

Asmita Parida [0009-0008-6935-9501](https://orcid.org/0009-0008-6935-9501)  
 Majesh Tomson [0000-0002-5492-1492](https://orcid.org/0000-0002-5492-1492)  
 ARUN K B [0000-0002-8292-5933](https://orcid.org/0000-0002-8292-5933)

## REFERENCES

- Abdelrahman, E.A., Hegazey, R.M., Ismail, S.H., El-Feky, H.H., Khedr, A.M., Khairy, M., Ammar, A.M., 2022. Facile synthesis and characterization of  $\beta$ -cobalt hydroxide/hydrohausmannite/ramsdellite/spertiniite and tenorite/cobalt manganese oxide/manganese oxide as novel nanocomposites for efficient photocatalytic degradation of methylene blue dye. *Arabian Journal of Chemistry* 15. <https://doi.org/10.1016/j.arabjc.2022.104372>
- Abelti, A.L., Abera Tekla, T., Fikreyesus Forsedo, S., Tamiru, M., Bultosa, G., Alkhtib, A., Burton, E., 2022. Bio-based smart materials for

- fish product packaging: a review. *International Journal of Food Properties* 25(1), 857–871. <https://doi.org/10.1080/10942912.2022.2066121>
- Al-Saidi, Al-Alawi, Rahman, Guizani, N., 2012. Fourier transform infrared (FTIR) spectroscopic study of extracted gelatin from shaari (*Lithrinus microdon*) skin: effects of extraction conditions, *International Food Research Journal* 19(3), 1167–1173
- Arpi, N., Fahrizal, F., Novita, M., 2018. Isolation of fish skin and bone gelatin from tilapia (*Oreochromis niloticus*): Response surface approach, in: IOP Conference Series: Materials Science and Engineering 334, 012061. <https://doi.org/10.1088/1757-899X/334/1/012061>
- Avena-Bustillos, R.J., Chiou, B., Olsen, C.W., Bechtel, P.J., Olson, D.A., Mchugh, T.H., 2011. Gelation, oxygen permeability, and mechanical properties of mammalian and fish gelatin films. *Journal of Food Science* 76(7), E519–E524. <https://doi.org/10.1111/j.1750-3841.2011.02312.x>
- Badawi, N.M., Attia, Y.M., El-Kersh, D.M., Hammam, O.A., Khalifa, M.K.A., 2022. Investigating the impact of optimized trans-cinnamic acid-loaded PLGA nanoparticles on epithelial to mesenchymal transition in breast cancer. *International Journal of Nanomedicine* 17, 4627–4643. <https://doi.org/10.2147/IJN.S345870>
- Bellon-Maurel, V., Aissani, L., Bessou, C., Lardon, L., Loiseau, E., Risch, E., Roux, P., Junqua, G., 2013. What scientific issues in life cycle assessment applied to waste and biomass valorization? Editorial. *Waste Biomass Valorization* 4. <https://doi.org/10.1007/s12649-012-9189-4>
- Bera, S., Xue, B., Rehak, P., Jacoby, G., Ji, W., Shimon, L.J.W., Beck, R., Král, P., Cao, Y., Gazit, E., 2020. Self-assembly of aromatic amino acid enantiomers into supramolecular materials of high rigidity. *ACS Nano* 14, 1694–1706. <https://doi.org/10.1021/acsnano.9b07307>
- Black, C.R., Berendzen, P.B., 2020. Shared ecological traits influence shape of the skeleton in flatfishes (Pleuronectiformes). *PeerJ* 8, e8919, 2020. <https://doi.org/10.7717/peerj.8919>
- Boran, G., Regenstein, J.M., 2010. Fish gelatin. *Advances in Food and Nutrition Research* 60, 119–143
- Campbell, H.D., 1983. The lowry protein assay: linearization of standard curve by double reciprocal plot. *Analytical Letters* 16(14), 1215–1224. <https://doi.org/10.1080/00032718308069542>
- Cheng, C., Tu, Z., Wang, H., 2023. pH-induced complex coacervation of fish gelatin and carboxylated chitosan: phase behavior and structural properties. *Food Research International* 167, 112652. <https://doi.org/10.1016/j.foodres.2023.112652>
- da Silva, L.C., Garcia, T., Mori, M., Sandri, G., Bonferoni, M.C., Finotelli, P. V., Cinelli, L.P., Caramella, C., Cabral, L.M., 2012. Preparation and characterization of polysaccharide-based nanoparticles with anticoagulant activity. *International Journal of Nanomedicine* 7, 2975–2986. <https://doi.org/10.2147/IJN.S31632>
- Das, M.P., R., S.P., Prasad, K., Jv, V., M, R., 2017. Extraction and characterization of gelatin: a functional biopolymer. *International Journal of Pharmacy and Pharmaceutical Sciences* 9(9), 239–242. <https://doi.org/10.22159/ijpps.2017v9i9.17618>
- Flieger, J., Flieger, M., 2020. The [DPPH•/DPPH-H]-HPLC-DAD method on tracking the antioxidant activity of pure antioxidants and goutweed (*Aegopodium podagraria* L.) hydroalcoholic extracts. *Molecules* 25(24), 6005. <https://doi.org/10.3390/MOLECULES25246005>
- Giménez, B., Gómez-Guillén, M.C., Montero, P., 2005. Storage of dried fish skins on quality characteristics of extracted gelatin. *Food Hydrocolloids* 19(16), 958–963. <https://doi.org/10.1016/j.foodhyd.2004.12.012>
- Gómez-Guillén, M.C., Giménez, B., Montero, P., n.d., 2002. Extraction of gelatin from fish skins by high pressure treatment. *Food Hydrocolloids* 16(1), 25–31. [https://doi.org/10.1016/S0268-005X\(01\)0005-9](https://doi.org/10.1016/S0268-005X(01)0005-9)
- Gonçalves, J., Luís, Â., Gallardo, E., Duarte, A.P., 2022. Evaluation of the in vitro wound-healing potential of Ayahuasca. *Molecules* 27(18), 5760. <https://doi.org/10.3390/molecules27185760>
- Gornall, J.L., Terentjev, E.M., 2008. Helix-coil transition of gelatin: Helical morphology and stability. *Soft Matter* 4(3), 544–549. <https://doi.org/10.1039/b713075a>
- Gould, L.J., Orgill, D.P., Armstrong, D.G., Galiano, R.D., Glat, P.M., Zelen, C.M., DiDomenico, L.A., Carter, M.J., Li, W.W., 2022. Improved healing of chronic diabetic foot wounds in a prospective randomised controlled multi-centre clinical trial with a microvascular tissue allograft. *International Wound Journal* 19(4), 901–913. <https://doi.org/10.1111/iwj.13679>
- Hagiwara, K., Kishimoto, S., Ishihara, M., Koyama, Y., Mazda, O., Sato, T., 2013. In vivo gene transfer using pDNA/chitosan/chondroitin sulfate ternary complexes: Influence of chondroitin sulfate on the stability of freeze-dried complexes and transgene expression in vivo. *Journal of Gene Medicine* 15(4), 139–148. <https://doi.org/10.1002/jgm.2694>
- Hall, B.G., 2013. Building phylogenetic trees from molecular data with MEGA. *Molecular Biology and Evolution* 30(5), 1229–1235. <https://doi.org/10.1093/molbev/mst012>
- Hemker, A.K., Nguyen, L.T., Karwe, M., Salvi, D., 2020. Effects of pressure-assisted enzymatic hydrolysis on functional and bioactive properties of tilapia (*Oreochromis niloticus*) by-product protein hydrolysates. *LWT* 122, 109003. <https://doi.org/10.1016/j.lwt.2019.109003>
- Hidayati, D., Sabiyla, G.R., Prasetyo, E.N., Sa'adah, N.N., Kurniawan, F., 2021. The characteristic of gelatin extracted from the skin of adult and sub-adult striped catfish (*Pangasius hypophthalmus*) using acid-base pretreatment: pH and FTIR, in: IOP Conference Series: Earth and Environmental Science 755, 012018. IOP Publishing Ltd. <https://doi.org/10.1088/1755-1315/755/1/012018>
- Huang, C.Y., Wu, T.C., Hong, Y.H., Hsieh, S.L., Guo, H.R., Huang, R.H., 2018. Enhancement of cell adhesion, cell growth, wound healing, and oxidative protection by gelatins extracted from extrusion-pretreated tilapia (*Oreochromis* sp.) fish scale. *Molecules* 23(10), 2406. <https://doi.org/10.3390/molecules23102406>
- Huang, T., Tu, Z. cai, Xincheng-Shangguan, Wang, H., Zhang, L., Sha, X. mei, 2017. Rheological and structural properties of fish scales gelatin: effects of conventional and ultrasound-assisted extraction. *International Journal of Food Properties* 20(Suppl. 3), S2535–S2547. <https://doi.org/10.1080/10942912.2017.1295388>
- Ibrahim, M., Mahmoud, A.A., Osman, O., Abd El-Aal, M., Eid, M., 2011. Molecular spectroscopic analyses of gelatin. *Spectrochimica Acta, Part A: Molecular and Biomolecular Spectroscopy* 81(1), 724–729. <https://doi.org/10.1016/J.SAA.2011.07.012>
- Jardim, K.V., Siqueira, J.L.N., Bão, S.N., Sousa, M.H., Parize, A.L., 2020. The role of the lecithin addition in the properties and cytotoxic activity of chitosan and chondroitin sulfate nanoparticles containing curcumin. *Carbohydrate Polymer* 227, 115351. <https://doi.org/10.1016/j.carbpol.2019.115351>
- Karydis-Messinis, A., Moschovas, D., Markou, M., Tsirka, K., Gioti, C., Bagli, E., Murphy, C., Giannakas, A.E., Paipetis, A., Karakassides, M.A., Avgeropoulos, A., Salmas, C.E., Zafeiropoulos, N.E., 2023. Hydrogel membranes from chitosan-fish gelatin-glycerol for biomedical applications: chondroitin sulfate incorporation effect in

- membrane properties. *Gels* 9(11), 844. <https://doi.org/10.3390/gels9110844>
- Katakami, C., Appel, A., Raymond, L.A., Lipman, M.J., Kao, W.W.Y., 1985. Synthesis of chondroitin sulfate by fibrotic vitreous induced by monocytes and lymphocytes. *Experimental Eye Research* 41(3), 357–369. [https://doi.org/10.1016/S0014-4835\(85\)80008-7](https://doi.org/10.1016/S0014-4835(85)80008-7)
- Kishipour, S., Teimori, A., Askari Hesni, M., Motamedi, M., 2023. Scale morphological variation across the flank in four Tonguefishes species collected from the Gulf of Oman (Pleuronectiforms; Cynoglossidae). *Acta Zoologica* 104(2), 302–314. <https://doi.org/10.1111/azo.12443>
- Knebelberger, T., Stöger, I., 2012. DNA extraction, preservation, and amplification. *Methods in Molecular Biology* 858, 311–338. [https://doi.org/10.1007/978-1-61779-591-6\\_14](https://doi.org/10.1007/978-1-61779-591-6_14)
- Konovalova, I., Novikov, V., Kuchina, Y., Dolgopiatova, N., 2020. Technology and properties of chondroitin sulfate from marine hydrobionts. *KnE Life Sciences* 5(1), 367–376. <https://doi.org/10.18502/cls.v5i1.6075>
- Krüzelyi, D., Ott, P.G., Móricz, Á.M., 2023. Exploring antioxidant potential in two basidiomycetous mushrooms using high-performance thin-layer chromatography–DPPH–videodensitometry. *Journal of Planar Chromatography - Modern TLC* 36(3), 247–255. <https://doi.org/10.1007/s00764-023-00271-y>
- Legler, G., Müller-Platz, C.M., Mentges-Hettkamp, M., Pflieger, G., Jülich, E., 1985. On the chemical basis of the Lowry protein determination. *Analytical Biochemistry* 150, 278–287. [https://doi.org/10.1016/0003-2697\(85\)90511-1](https://doi.org/10.1016/0003-2697(85)90511-1)
- Malik, F., Malaka, M.H., Fristiohady, A., Wahyuni, W., Hamsid, R., Sahidin, S., Gani, A.F., 2022. Cytotoxic activity of Kasumba flower ethanol extract turate (*Carthamus tinctorius* Linn.) against the line of cancer cells T47D breasts. *Jurnal Farmasi Sains dan Praktis* 7(3), 233–240. <https://doi.org/10.31603/pharmacy.v7i3.6113>
- Mao, J.J., Rahemtulla, F., Scott, P.G., 1998. Proteoglycan expression in the rat temporomandibular joint in response to unilateral bite raise. *Journal of Dental Research* 77(7), 1520–1528. <https://doi.org/10.1177/00220345980770070701>
- Medeiros, L.H.C., Vasconcelos, B.M.F., Silva, M.B., Souza-Junior, A.A., Chavante, S.F., Andrade, G.P.V., 2021. Chondroitin sulfate from fish waste exhibits strong intracellular antioxidant potential. *Brazilian Journal of Medical and Biological Research* 54(3), e10730. <https://doi.org/10.1590/1414-431X2020E10730>
- Minicozzi, M.R., Perez, J., Kimball, D.S., Gibb, A.C., 2019. Scale thickness predicts skin puncture-force resistance in three pleuronectiform fishes. *Integrative Organismal Biology* 1(1), obz005. <https://doi.org/10.1093/iob/obz005>
- Muchová, J., Hearnden, V., Michlovská, L., Vištejnová, L., Zavadáková, A., Šmerková, K., Kočiová, S., Adam, V., Kopel, P., Vojtová, L., 2021. Mutual influence of selenium nanoparticles and FGF2-STAB® on biocompatible properties of collagen/chitosan 3D scaffolds: in vitro and ex ovo evaluation. *Journal of Nanobiotechnology* 19, 103. <https://doi.org/10.1186/s12951-021-00849-w>
- Nandiyanto, A.B.D., Oktiani, R., Ragadhita, R., 2019. How to read and interpret FTIR spectroscopy of organic material. *Indonesian Journal of Science and Technology* 4(1), 97–118. <https://doi.org/10.17509/ijost.v4i1.15806>
- Neuman, R.E., Logan, M.K., n.d. The determination of hydroxyproline. *Journal of Biological Chemistry* 184(1), 299–306. [https://doi.org/10.1016/S0021-9258\(19\)51149-8](https://doi.org/10.1016/S0021-9258(19)51149-8)
- Nithinkumar, G.N., Rao, V.A., Babu, R.N., Kannan, T.A., 2022. Extraction and physico-chemical properties of chondroitin sulphate from bovine trachea. *Indian Veterinary Journal* 99(4), 33–36.
- Nogueira, A. V., Rossi, G.R., Iacomini, M., Sasaki, G.L., Trindade, E.S., Cipriani, T.R., 2019. Viscera of fishes as raw material for extraction of glycosaminoglycans of pharmacological interest. *International Journal of Biological Macromolecules* 121, 544–550. <https://doi.org/10.1016/j.ijbiomac.2018.09.156>
- Nzihou, A., 2010. Toward the valorization of waste and biomass. *Waste Biomass Valorization* 1(1), 3–7. <https://doi.org/10.1007/s12649-010-9014-x>
- Oliveira, L.C. de, Barbosa, J.R., Ribeiro, S. da C.A., Vasconcelos, M.A.M. de, Aguiar, B.A. de, Pereira, G.V. da S., Albuquerque, G.A., Silva, F.N.L. da, Crizel, R.L., Campelo, P.H., Lourenço, L. de F.H., 2019. Improvement of the characteristics of fish gelatin – gum arabic through the formation of the polyelectrolyte complex. *Carbohydrate Polymer* 223, 115068. <https://doi.org/10.1016/j.carbpol.2019.115068>
- Oujifard, A., Bagheri, D., Shadi, A., Hosseini, S.J., Kiani, N., 2017. Morphometric variation of large scale tongue sole *Cynoglossus arel* (Bloch & Schneider, 1801) in the north of Persian Gulf. *Journal of Applied Ichthyological Research* 5, 19–30.
- Peterson, G.L., 1979. Review of the folin phenol protein quantitation method of lowry, rosebrough, farr and randall. *Analytical Biochemistry* 100, 201–220. [https://doi.org/10.1016/0003-2697\(79\)90222-7](https://doi.org/10.1016/0003-2697(79)90222-7)
- Pezeshki-Modaress, M., Mirzadeh, H., Zandi, M., Rajabi-Zeleti, S., Sodeifi, N., Aghdami, N., Mofrad, M.R.K., 2017. Gelatin/chondroitin sulfate nanofibrous scaffolds for stimulation of wound healing: In-vitro and in-vivo study. *Journal of Biomedical Materials Research A* 105(7), 2020–2031. <https://doi.org/10.1002/jbm.a.35890>
- Pijuan, J., Barceló, C., Moreno, D.F., Maiques, O., Sisó, P., Martí, R.M., Macià, A., Panosa, A., 2019. In vitro cell migration, invasion, and adhesion assays: from cell imaging to data analysis. *Frontiers in Cell and Developmental Biology* 7, 107. <https://doi.org/10.3389/fcell.2019.00107>
- Pomory, C.M., 2008. Color development time of the Lowry protein assay. *Analytical Biochemistry* 378(2), 216–217. <https://doi.org/10.1016/j.ab.2008.04.015>
- Rajabimashhadi, Z., Gallo, N., Salvatore, L., Lionetto, F., 2023. Collagen derived from fish industry waste: progresses and challenges. *Polymers (Basel)* 15(3), 544. <https://doi.org/10.3390/polym15030544>
- Redmile-Gordon, M.A., Armenise, E., White, R.P., Hirsch, P.R., Goulding, K.W.T., 2013. A comparison of two colorimetric assays, based upon Lowry and Bradford techniques, to estimate total protein in soil extracts. *Soil Biology and Biochemistry* 67, 166–173. <https://doi.org/10.1016/j.soilbio.2013.08.017>
- Ribeiro, T.G., Chávez-Fumagall, M.A., Valadares, D.G., França, J.R., Rodrigues, L.B., Duarte, M.C., Lage, P.S., Andrade, P.H.R., Lage, D.P., Arruda, L. V., Refidaff, C., Costa, L.E., Martins, V.T., Tavares, C.A.P., Castilho, R.O., Coelho, E.A.F., Faraco, A.A.G., 2014. Novel targeting using nanoparticles: an approach to the development of an effective anti-leishmanial drug-delivery system. *International Journal of Nanomedicine* 9, 877–890. <https://doi.org/10.2147/IJN.S55678>
- Rocha-Pimienta, J., Navajas-Preciado, B., Barraso-Gil, C., Martillanes, S., Delgado-Adámez, J., 2023. Optimization of the extraction of chitosan and fish gelatin from fishery waste and their antimicrobial potential as active biopolymers. *Gels* 9(3), 254. <https://doi.org/10.3390/gels9030254>

- Saftić Martinović, L., Birkic, N., Miletić, V., Antolović, R., Štanfel, D., Wittine, K., 2023. Antioxidant activity, stability in aqueous medium and molecular docking/dynamics study of 6-amino- and n-methyl-6-amino-l-ascorbic acid. *International Journal of Molecular Sciences* 24(2), 1410. <https://doi.org/10.3390/ijms24021410>
- See, S.F., Ghassem, M., Mamot, S., Babji, A.S., 2015. Effect of different pretreatments on functional properties of African catfish (*Clarias gariepinus*) skin gelatin. *Journal of Food Science and Technology* 52(11), 7530–7539. <https://doi.org/10.1007/s13197-013-1043-6>
- Seixas, M.J., Martins, E., Reis, R.L., Silva, T.H., 2020. Extraction and characterization of collagen from elasmobranch byproducts for potential biomaterial use. *Marine Drugs* 18(12), 617. <https://doi.org/10.3390/md18120617>
- Sen, D.P., Rao, T.S.S., Lahiry, N.L., 1966. Defatting and deodorization of fish protein concentrate from Harpodon Nehereus. *Journal of Food Science* 3(5), 673–677. <https://doi.org/10.1111/j.1365-2621.1966.tb00504.x>
- Serrano-Lotina, A., Portela, R., Baeza, P., Alcolea-Rodriguez, V., Villaruel, M., Ávila, P., 2023. Zeta potential as a tool for functional materials development. *Catalysis Today* 423, 114160. <https://doi.org/10.1016/j.cattod.2022.08.004>
- Shiao, W.C., Wu, T.C., Kuo, C.H., Tsai, Y.H., Tsai, M.L., Hong, Y.H., Huang, C.Y., 2021. Physicochemical and antioxidant properties of gelatin and gelatin hydrolysates obtained from extrusion-pretreated fish (*Oreochromis* sp.) scales. *Marine Drugs* 19(5), 275. <https://doi.org/10.3390/md19050275>
- Sikder, S.K., Das, A., 1979. Isolation and characterization of glycosaminoglycans (mucopolysaccharides) from the skin of the fish *Labeo rohita*. *Carbohydrate Research* 71(1), 79–86. [https://doi.org/10.1016/S0008-6215\(00\)86075-9](https://doi.org/10.1016/S0008-6215(00)86075-9)
- Soltani, M., Haghbin Nazarpak, M., Zamani, A., Solouk, A., 2023. Evaluation of curcumin release from wound dressing based on gelatin and sturgeon-derived chondroitin sulfate. *Materials Today Communications* 35, 106167. <https://doi.org/10.1016/j.mtcomm.2023.106167>
- Soman, C., Anjaneyappa, H.N., Kumar, B.T.N., Devanand, T.N., Sathish, R.P., Shekar, M., 2020. DNA barcoding of *Cynoglossus arel* using mitochondrial COI and 16S rRNA genes. *Indian Journal of Animal Sciences* 90(7), 1010–1013. <https://doi.org/10.56093/ijans.v90i7.106685>
- Tamura, K., Peterson, D., Peterson, N., Stecher, G., Nei, M., Kumar, S., 2011. MEGA5: Molecular evolutionary genetics analysis using maximum likelihood, evolutionary distance, and maximum parsimony methods. *Molecular Biology and Evolution* 28(10), 2731–2739. <https://doi.org/10.1093/molbev/msr121>
- Tekle, S., Bozkurt, F., Akman, P.K., Sagdic, O., 2022. Bioactive and functional properties of gelatin peptide fractions obtained from sea bass (*Dicentrarchus labrax*) skin. *Food Science and Technology (Brazil)* 42, e60221. <https://doi.org/10.1590/ft.60221>
- Thomas, L., Kp, M., Mathew, S., 2021. Fish gills of *Thunnus albacares*: A novel source of chondroitin sulphate glycosaminoglycans. *International Journal of Fisheries and Aquatic Studies* 9(3), 146–150.
- Tkachenko, Y., Niedzielski, P., 2022. FTIR as a method for qualitative assessment of solid samples in geochemical research: a review. *Molecules* 27(24), 8846. <https://doi.org/10.3390/molecules27248846>
- Vázquez, J.A., Fraguas, J., Novoa-Carballal, R., Reis, R.L., Pérez-Martín, R.I., Valcarcel, J., 2019. Optimal isolation and characterization of chondroitin sulfate from rabbit fish (*Chimaera monstrosa*). *Carbohydrate Polymers* 210, 302–313. <https://doi.org/10.1016/j.carbpol.2019.01.075>
- Volpi, N., Maccari, F., Titze, J., 2005. Simultaneous detection of sub-microgram quantities of hyaluronic acid and dermatan sulfate on agarose-gel by sequential staining with toluidine blue and Stains-All. *Journal of Chromatography B, Analytical Technologies in the Biomedical and Life Sciences* 820(1), 131–135. <https://doi.org/10.1016/j.jchromb.2005.03.028>
- Wang, W., Wang, K., Guo, Y., Zhang, C., Li, P., Liu, H., 2023. Efficient extraction and structural characterization of chondroitin sulfate by deep eutectic solvents. *Nongye Gongcheng Xuebao/Transactions of the Chinese Society of Agricultural Engineering* 39(23), 276–284. <https://doi.org/10.11975/j.issn.1002-6819.202307268>
- Wang, Y., Regenstein, J.M., 2009. Effect of EDTA, HCl, and citric acid on Ca salt removal from Asian (silver) carp scales prior to gelatin extraction. *Journal of Food Science* 74(6), C426–C431. <https://doi.org/10.1111/j.1750-3841.2009.01202.x>
- Wu, J., Xiao, J., Zhu, M., Yang, H., Liu, J., Liu, Y., 2023. Study of physicochemical and gelation properties of fish gelatin from different sources. *Applied Sciences (Switzerland)* 13(9), 5337. <https://doi.org/10.3390/app13095337>
- Ye, J., Huang, B., Gong, P., 2021. Nerve growth factor-chondroitin sulfate/hydroxyapatite-coating composite implant induces early osseointegration and nerve regeneration of peri-implant tissues in Beagle dogs. *Journal of Orthopaedic Surgery and Research* 16, 77. <https://doi.org/10.1186/s13018-020-02177-5>
- Zhou, P., Regenstein, J.M., 2006. Determination of total protein content in gelatin solutions with the Lowry or Biuret assay. *Journal of Food Science* 71(8), C474–C479. <https://doi.org/10.1111/j.1750-3841.2006.00151.x>